Recovering High-Order Accuracy in Nonlinear Caputo Systems by Correcting Initial Singularities

Butta Shivaprasad[1], Prof. (Dr.) Vishal Saxena[2], Dr. Rachana Khandelwal[3]
[1]*Research Scholar, Department of Mathematics, Jayoti Vidyapeeth Women's University, Jaipur, Rajasthan, India*
[2]*Supervisor, Department of Mathematics, Jayoti Vidyapeeth Women's University, Jaipur, Rajasthan, India*
[3]*Co-supervisor, Department of Mathematics, Jayoti Vidyapeeth Women's University, Jaipur, Rajasthan, India*

***Abstract*—Weak initial singularities can sharply reduce the accuracy of numerical schemes for nonlinear Caputo systems, even when the interpolant is quadratic. This study examines a block-implicit product-integration method on a uniform mesh and tests a correction that integrates a known fractional-power term analytically. A finite-horizon contraction argument gives unique discrete solvability and a third-order maximum nodal error bound when the right-hand side along the exact solution, after correction where needed, has three bounded time derivatives. Manufactured nonlinear scalar benchmarks at fractional orders 0.4, 0.7 and 0.9 show final refinement rates of 0.802–1.802 without correction and 3.385–3.939 with correction. At order 0.7 and 128 panels, the correction reduces maximum nodal error from 3.061×10^{-5} to 8.925×10^{-10}. The analysis distinguishes errors caused by limited initial regularity from those due to the nonlinear stage solve. The experiments establish the effect of exact singular-term subtraction on these benchmarks and identify coefficient estimation and work-normalised comparison as priorities for practical applications.**

***Index Terms*—Caputo derivative, product integration, initial singularity, nonlinear systems, convergence, manufactured solutions**

Scope of Future Research:
The next tests should perturb the singular coefficient, compare corrections with graded meshes under a common work budget, and include genuinely coupled stiff systems. Long-time discrete stability requires a separate analysis of the numerical recurrence.

Research Outcomes for Scientific Computing:
The error bound, exact trajectories and tabulated refinement rates give researchers and scientific-software developers a benchmark for checking whether an implementation captures the expected accuracy when a dominant starting singularity is present.

I. INTRODUCTION AND BACKGROUND OF THE PROBLEM

A numerical solution of a fractional initial-value problem is used to represent a trajectory whose evolution depends on its entire history. In the Volterra representation of the Caputo problem, the kernel is integrable but becomes singular at the evaluation time. Product integration addresses this feature by integrating the kernel against polynomial basis functions. A second difficulty occurs at the initial time, where fractional powers can make the solution or its associated right-hand side insufficiently smooth for high-order interpolation. These two singularities enter the analysis in different places. Kernel integration handles the singular upper limit, while initial regularity controls the interpolation defect.
The study asks whether exact subtraction of a known starting term recovers high-order accuracy for one quadratic product-integration discretisation. The comparison uses the same nonlinear equation and time grid for the corrected and uncorrected runs. The correction therefore isolates the contribution of the initial fractional term, while a smooth manufactured problem provides a separate check of the

implementation. The analytical objective is an explicit finite-horizon estimate that accounts for the error left by the nonlinear solver.

Problem Statement:

Quadratic product integration offers a third-order nodal bound under a smoothness condition, but Caputo dynamics can violate that condition at the first panel. The problem is to determine which part of that loss can be recovered by integrating the leading nonsmooth term exactly, and to establish the assumptions under which the recovered accuracy follows from the discrete equations.

II. REVIEW OF LITERATURE

Lubich (1986) developed a systematic discretised fractional calculus based on convolution weights. Brunner (2004) established the collocation framework for Volterra integral equations, including weakly singular problems. Diethelm et al. (2004) analysed fractional Adams errors, and Diethelm (2010) developed the integral formulation and analysis of Caputo initial-value problems.

Stynes et al. (2017) showed how initial regularity and mesh grading affect convergence in a time-fractional diffusion problem. Their setting motivates the present regularity comparison. Garrappa (2018) reviewed practical methods for fractional differential equations, including product-integration schemes and the treatment of persistent history. Here the quadrature construction is used to quantify how subtracting a known singular contribution changes error for a fixed uniform-grid method.

III. MATERIALS AND METHODS

3.1 Integral Formulation and Interpolation

Let $0 < \alpha < 1$, with a common order α for each component of $u \in \mathbb{R}^d$. Write the initial-value problem as a Volterra equation with initial value u_0 and right-hand side f.

$$u(t) = u_0 + \frac{1}{\Gamma(\alpha)} \int_0^t (t-s)^{\alpha-1} f\big(s, u(s)\big)\, ds \qquad (1)$$

Divide [0, T] into N panels of length h. Set $t_j = jh$ and let $v = (s - t_j)/h$ on panel j. The right-hand side is interpolated at v = 0, 1/2 and 1 using the three Lagrange polynomials below.

$$\ell_0(v) = 1 - 3v + 2v^2, \quad \ell_1(v) = 4v - 4v^2, \quad \ell_2(v) = -v + 2v^2 \quad (2)$$

3.2 Weights and Coupled Stage Equations

At target $t = t_n + ch$, take $c \in \{1/2, 1\}$, $a = n - j + c$ and $b = 1$ on completed panels or $b = c$ on the current panel. The polynomial weights and the two stage equations are

$$W_{jk}(t) = \frac{h^\alpha}{\Gamma(\alpha)} \int_0^b (a-v)^{\alpha-1} \ell_k(v)\, dv \qquad (3)$$

$$U_{n,c} = u_0 + \sum_{j=0}^{n} \sum_{k=0}^{2} W_{jk}\,(t_n + ch) F_{jk}, \quad c \in \{1/2, 1\} \quad (4)$$

Here F_{jk} is f evaluated at the time and numerical stage corresponding to node k on panel j. Its left endpoint is inherited from the previous panel. For the midpoint target, the current-panel polynomial depends on the new endpoint value. As a result, the midpoint and endpoint are solved together in a nonlinear system of dimension 2d.

Writing each basis polynomial as a sum of monomials reduces the weights to integrals of $v^r(a - v)^{\wedge}(\alpha-1)$, with r = 0, 1, 2. For a = b, these equal $b^{\wedge}(r+\alpha)$ B(r + 1, α), where B is the beta function. For the smooth historical weights, the source calculations used adaptive integration with absolute tolerance 2×10^{-12} before scaling by $h^{\wedge}\alpha/\Gamma(\alpha)$. The lag weights were precomputed, and the nonlinear root solver used the previous endpoint to initialise both new stages. For fixed stage-solve cost per panel, the direct history summation uses $O(N^2 d)$ arithmetic and $O(Nd)$ stored stages.

3.3 Solvability and Maximum Nodal Error

Assume f is globally Lipschitz in u with constant L in the maximum norm. For the exact trajectory define g(t) = f(t, u(t)). If g has three bounded derivatives and M_3 bounds the third derivative, the Lagrange remainder gives

$$\| g - \Pi_2 g \|_\infty \le C_3 h^3, \quad C_3 = \frac{M_3}{72\sqrt{3}} \qquad (5)$$

The constant follows from the maximum of |v(v − 1/2)(v − 1)|, which is 1/(12√3). Integrating the interpolation defect against the positive fractional kernel gives a nodal defect of at most $C_3 h^3 T^\alpha/\Gamma(1+\alpha)$. The Lebesgue constant of the basis is 5/4. On the first half of the panel the sum of the absolute basis values is $1 + 2v - 4v^2$, with the second half obtained by symmetry.

$$Q = \frac{5LT^\alpha}{4\Gamma(1+\alpha)} \qquad (6)$$

Proposition. If $Q < 1$, the ideal discrete equations have a unique solution. For any approximate stage vector with maximum algebraic residual bounded by ρ_h in the ideal equations, its maximum nodal error E_h satisfies

$$E_h \le \frac{C_3 h^3 T^\alpha/\Gamma(1+\alpha) + \rho_h}{1 - Q} \qquad (7)$$

Proof. The absolute weight sum is bounded by the fractional integral of the basis Lebesgue function, so the discrete map has Lipschitz constant at most Q. Banach's fixed-point theorem gives existence and uniqueness. Subtracting the approximate stage equations from the exact nodal identity yields an error bounded by the interpolation defect, Q E_h and ρ_h. Solving the inequality gives (7). The result yields third order if $\rho_h = O(h^3)$. For floating-point weights, their evaluation error adds a separate defect to the numerator.

3.4 Initial Singularity Correction

Suppose the exact right-hand side contains a known term $S(t) = a\, t^\sigma$ with $\sigma > -1$. Subtract S(t) from f before interpolating and add its exact fractional integral at each target. The analytic contribution is $a\Gamma(\sigma+1)t^{\sigma+\alpha}/\Gamma(\sigma+\alpha+1)$. This representation leaves the Volterra equation unchanged. The corrected right-hand side has the same Lipschitz constant in u, and the error estimate applies if the remaining exact time dependence has three bounded derivatives.

The correction is sensitive to its coefficient. If the same power t^σ is subtracted with coefficient â, the residual still contains $(a - \hat{a})t^\sigma$. For $0 < \sigma < 1$ this term has an unbounded first derivative at the origin unless the coefficients agree. Thus an inaccurate coefficient can reduce the size of the singular contribution while leaving the regularity hypothesis unsatisfied. This observation motivates a coefficient-sensitivity study with deliberately perturbed values.

3.5 Manufactured Verification Problems

The scalar experiments set T = 1, η = 0.2 and α ∈ {0.4, 0.7, 0.9}. The smooth solution is $u_s(t) = 1 + t^4$. The initially singular solution is

$$u_w(t) = 1 + t^\alpha + t^{2\alpha} + t^4 \qquad (8)$$

Both are imposed as exact trajectories by using their Caputo derivatives and a nonlinear state perturbation.

$$f(t,u) = D^\alpha_{C,0} u_{\text{exact}}(t) + \eta\big[\tanh(u) - \tanh\big(u_{\text{exact}}(t)\big)\big] \qquad (9)$$

The perturbation vanishes on the prescribed trajectory and has $L \le 0.2$. This gives Q approximately 0.282, 0.275 and 0.260 at the three tested orders, respectively. For the singular solution, the Caputo derivative is the sum of $\Gamma(1+\alpha)$, $[\Gamma(1+2\alpha)/\Gamma(1+\alpha)]t^\alpha$ and $24t^{4-\alpha}/\Gamma(5-\alpha)$. The correction integrates the middle term exactly to $t^{2\alpha}$. The remainder has three bounded derivatives because $4 - \alpha > 3$.

Each variant uses N ∈ {8, 16, 32, 64, 128}. The quadratic method measures the maximum error over panel endpoints and midpoints. The observed order is $\log_2(E_n/E_{2n})$, where E_n is the maximum error on the N-panel grid. For the corrected singular case at α = 0.7, an implicit linear product-integration baseline uses the same panel counts and evaluates the error at endpoints. The reported calculations use double precision with Python, NumPy and SciPy.

Table 1. Maximum nodal error under mesh refinement at α = 0.7

Panels N	Smooth error	Uncorrected error	Corrected error	Corrected rate
8	2.9408e-05	1.5094e-03	2.8839e-05	—
16	2.1768e-06	5.6563e-04	2.1381e-06	3.754
32	1.6175e-07	2.1365e-04	1.5908e-07	3.748
64	1.2075e-08	8.0840e-05	1.1889e-08	3.742
128	9.0558e-10	3.0607e-05	8.9245e-10	3.736

Source. Manufactured-solution computations in the original manuscript.

IV. RESULTS AND DISCUSSION

Table 2. Maximum errors and final refinement rates at 128 panels

Order α	Case	Maximum error	Last rate
0.4	smooth	4.6277e-09	3.384
0.4	singular uncorrected	1.2761e-03	0.802
0.4	singular corrected	4.6607e-09	3.385
0.7	smooth	9.0558e-10	3.737
0.7	singular uncorrected	3.0607e-05	1.401
0.7	singular corrected	8.9245e-10	3.736
0.9	smooth	3.3865e-10	3.940
0.9	singular uncorrected	1.2155e-06	1.802
0.9	singular corrected	3.3160e-10	3.939

For the uncorrected singular trajectory, the final observed orders are very close to 2α at all three tested α values. This is consistent with the t^α term in the integrand contributing on the scale h^(2α) at the first panel after fractional integration. The comparisons reported here measure global nodal errors, so the first-panel scaling is an explanation consistent with the data rather than a global asymptotic proof.

At α = 0.7 and N = 128, the correction reduces maximum nodal error by approximately 34,300 times. Corrected and smooth rates lie close to one another across all three orders. The computed rates above three describe these manufactured trajectories and tested meshes. The uniform estimate established in Section 3.3 guarantees third order under its stated assumptions.

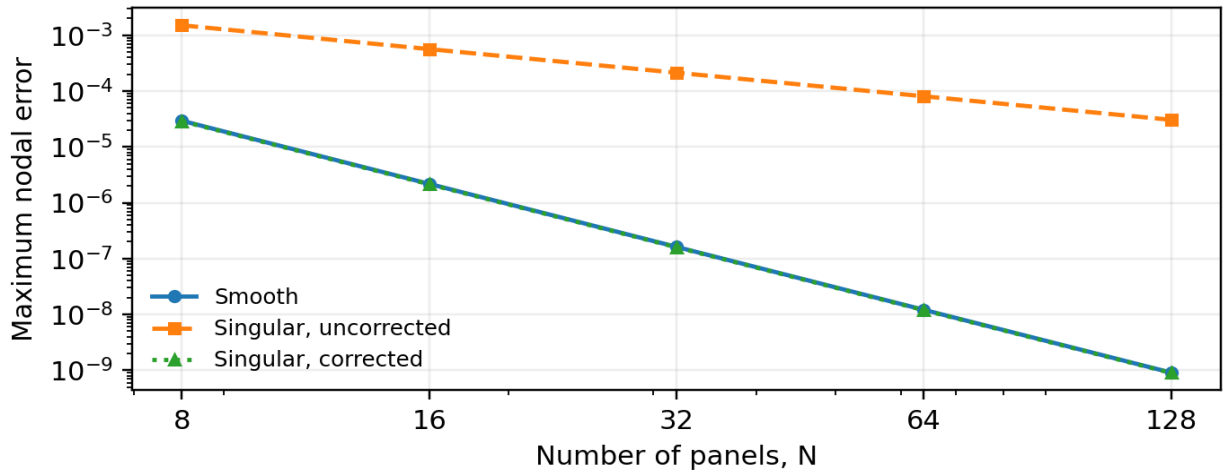

Figure 1. Maximum nodal error at α = 0.7 on logarithmic axes. Source: Table 1.

The maximum nonlinear stage residual reported over the 45 quadratic runs is 1.0214×10^{-14}. This is over four orders of magnitude below the smallest reported trajectory error. The residual therefore supports the interpretation that the measured differences arise chiefly from discretisation and regularity in the tested cases. The computation itself has no interval enclosure for weight or rounding errors.

Table 3. Linear and quadratic product integration on the corrected case at α = 0.7

Panels N	Linear endpoint error	Linear rate	Quadratic all-node error
8	1.4989e-02	—	2.8839e-05
16	3.8151e-03	1.974	2.1381e-06
32	9.6353e-04	1.985	1.5908e-07

64	2.4233e-04	1.991	1.1889e-08
128	6.0801e-05	1.995	8.9245e-10

Source. Manufactured-solution computations reported in the original manuscript.

The linear baseline has a final rate of 1.995. At the same panel count, the quadratic method remains more accurate despite measuring the error on a grid with additional midpoint samples. The methods solve different numbers of stage unknowns, and the available results do not establish an efficiency ranking. A work-normalised comparison would track function evaluations, nonlinear iterations, wall time and stored history alongside errors measured on a common set of times.

The benchmarks use a scalar, weakly nonlinear problem with an exactly known singular coefficient. The theoretical argument applies to commensurate finite-dimensional systems subject to its assumptions. Numerical transfer to coupled or stiff systems, misestimated starting coefficients and long integration windows remains open. The condition $Q < 1$ is sufficient and depends on T. It supplies no asymptotic stability region for a time-discrete equilibrium.

V. CONCLUSION

The experiments show that correcting a known starting singularity can recover high-order accuracy for quadratic product integration on a uniform mesh. The finite-horizon proof gives a third-order nodal error bound for the smooth remainder and makes the effect of the stage residual explicit. At $\alpha = 0.7$, the corrected error at 128 panels was approximately 8.925×10^{-10}, compared with 3.061×10^{-5} without correction. The result defines a concrete verification target for Caputo solvers and provides a basis for testing corrections when initial singular terms must be estimated.

REFERENCES

[1] Brunner, H. (2004). Collocation methods for Volterra integral and related functional differential equations. Cambridge University Press. https://doi.org/10.1017/CBO9780511543234

[2] Diethelm, K. (2010). The analysis of fractional differential equations: An application-oriented exposition using differential operators of Caputo type. Springer. https://doi.org/10.1007/978-3-642-14574-2

[3] Diethelm, K., Ford, N. J., & Freed, A. D. (2004). Detailed error analysis for a fractional Adams method. Numerical Algorithms, 36, 31–52. https://doi.org/10.1023/B:NUMA.0000027736.85078.be

[4] Garrappa, R. (2018). Numerical solution of fractional differential equations: A survey and a software tutorial. Mathematics, 6(2), Article 16. https://doi.org/10.3390/math6020016

[5] Lubich, C. (1986). Discretized fractional calculus. SIAM Journal on Mathematical Analysis, 17(3), 704–719. https://doi.org/10.1137/0517050